

Climatic Sensitivity of Dryland Soil CO₂ Fluxes Differs Dramatically with Biological Soil Crust Successional State

Colin L. Tucker,^{1*} Scott Ferrenberg,^{1,2} and Sasha C. Reed¹

¹Southwest Biological Science Center, US Geological Survey, 2290 SW Resource Blvd, Moab, Utah 84532, USA; ²Department of Biology, New Mexico State University, P.O. Box 30001, MSC 3AF, Las Cruces, New Mexico 88003, USA

ABSTRACT

Arid and semiarid ecosystems make up approximately 41% of Earth's terrestrial surface and are suggested to regulate the trend and interannual variability of the global terrestrial carbon (C) sink. Biological soil crusts (biocrusts) are common dryland soil surface communities of bryophytes, lichens, and/or cyanobacteria that bind the soil surface together and that may play an important role in regulating the climatic sensitivity of the dryland C cycle. Major uncertainties exist in our understanding of the interacting effects of changing temperature and moisture on CO₂ uptake (photosynthesis) and loss (respiration) from biocrust and sub-crust soil, particularly as related to biocrust successional state. Here, we used a mesocosm approach to assess how biocrust successional states related to climate treatments. We subjected bare soil (Bare), early successional lightly pigmented cyanobacterial biocrust (Early), and late successional darkly pigmented moss-lichen biocrust (Late) to either ambient or + 5°C above ambient

soil temperature for 84 days. Under ambient temperatures, Late biocrust mesocosms showed frequent net uptake of CO₂, whereas Bare soil, Early biocrust, and warmed Late biocrust mesocosms mostly lost CO₂ to the atmosphere. The inhibiting effect of warming on CO₂ exchange was a result of accelerated drying of biocrust and soil. We used these data to parameterize, via Bayesian methods, a model of ecosystem CO₂ fluxes, and evaluated the model with data from an autochamber CO₂ system at our field site on the Colorado Plateau in SE Utah. In the context of the field experiment, the data underscore the negative effect of warming on fluxes both biocrust CO₂ uptake and loss—which, because biocrusts are a dominant land cover type in this ecosystem, may extend to ecosystem-scale C cycling.

Key words: Bayesian statistics; biological soil crust; ecosystem model; gross primary production; moisture sensitivity; net soil exchange; semiarid shrublands; soil respiration; temperature sensitivity.

Received 20 October 2017; accepted 14 March 2018;
published online 30 April 2018

Electronic supplementary material: The online version of this article (<https://doi.org/10.1007/s10021-018-0250-4>) contains supplementary material, which is available to authorized users.

Author's Contribution: CT, SF, and SCR planned and designed the research. CT and SF performed field and laboratory work. CT analyzed data. CT, SF and SCR wrote the manuscript.

*Corresponding author; e-mail: ctucker@usgs.gov

HIGHLIGHTS

- Warming and associated drying reduce CO₂ fluxes from biocrusted soils.
- Moss-lichen biocrust fix more CO₂ than earlier successional states.
- A framework for biocrust C cycling response to climate change is presented.

INTRODUCTION

Arid and semiarid ecosystems represent our planet's largest biome (Schimel 2010), making up approximately 41% of Earth's land surface (Safriel and Adeel 2005) and may regulate both the long-term trajectory and interannual variability of the global terrestrial carbon (C) sink (Ahlström and others 2015). Given the low C density of dryland ecosystems, this strong role in global C cycling may seem surprising, but alongside their vast spatial extent, arid and semiarid ecosystems are highly responsive to climate variability (for example, Poulter and others 2014). The pulse-dynamic nature of dryland biotic processes suggests these ecosystems can respond rapidly to climate changes (for example, Austin and others 2004; Maestre and others 2012b). Increasing research effort has focused on elucidating interactions between the climate system and dryland C cycling, and improving our limited quantitative understanding of variability in dryland CO₂ flux and storage (Wohlfahrt and others 2008; Schlesinger and others 2009). Nevertheless, our understanding of the dryland C cycle at many scales remains conspicuously limited by our understanding of the components of biotic CO₂ exchange (for example, from soil microbes, vascular plants, and biological soil crusts) and how they are controlled by climatic drivers (for example, Sancho and others 2016).

Biological soil crusts (biocrusts) are communities of cyanobacteria, bryophytes, and/or lichens that bind soil together in a matrix resistant to wind and water erosion. Biocrusts are a major land cover type in drylands worldwide (Belnap and others 2016). These communities create a thin surface layer of high biotic and biogeochemical activity [that is, a 'mantle of fertility' (Garcia-Pichel and others 2003)], particularly within interspaces between perennial plants. The activities of biocrusts are fundamental to dryland biogeochemical cycles, including photosynthesis and respiration (Housman and others 2006; Darrouzet-Nardi and others 2015), N₂ fixation (reviewed in Barger and others

2016), gaseous nitrogen (N) release (Weber and others 2015), and internal N recycling (for example, Reed and others 2012). Biocrust organisms also can strongly affect surface temperature and albedo (Couradeau and others 2016; Rutherford and others 2017). Yet our understanding of biocrust biogeochemistry in a changing climate remains notably poor. Limited representation of biocrusts in our models of dryland ecosystem function constrains our understanding and prognostic capacity of the role drylands play in the Earth system (Ferrenberg and others 2017b; Barger and others 2016; Sancho and others 2016).

Several facts suggest biocrusts contribute to the total ecosystem C flux in drylands (Housman and others 2006; Castillo-Monroy and others 2011a; Elbert and others 2012; Sancho and others 2016). First, biocrusts may represent upwards of 70% of land cover in some regions (Belnap 1995); thus, even low respiration or photosynthesis rates could be magnified by high coverage compared to sparse vegetation. In deserts globally, biocrusts potentially contribute 9% of net primary production (Elbert and others 2012). Second, unlike vascular plants, biocrusts are not seasonally senescent or dormant and may utilize water pulses, including water vapor, at any time of year (Jasoni and others 2005; Darrouzet-Nardi and others 2015; McHugh and others 2015). This fact has mixed consequences for biocrust C balance: small water pulses during hot periods may cause C loss as respiration outpaces photosynthesis (Coe and others 2012; Reed and others 2012), whereas net C assimilation by biocrusts occurs during cool, wet, and even snowy periods (Darrouzet-Nardi and others 2015), and highest C uptake may occur only after several sequential wetting events (Burgheimer and others 2006). Finally, N₂ fixation by biocrusts may increase productivity of nearby vegetation in N-limited drylands (Pendleton and others 2003; Zhang and others 2016; Ferrenberg and others 2017a).

Biocrusts of different successional states differentially regulate key ecosystem functions (for example, Zaady and others 2000; Belnap 2002; Housman and others 2006; Grote and others 2010; Sancho and others 2016; Zhao and others 2016). In our study region, the Colorado Plateau in the USA, lightly pigmented, filamentous cyanobacterial biocrust (primarily composed of *Microcoleus vaginatus*) colonizes first following surface disturbance by trampling, wind or water driven erosion. Absent of repeated disturbance, moss (for example, *Syntrichia caninervis*, *Syntrichia ruralis*), and lichen (for example, *Collema tenax*, *Aspicilia* spp., *Peltula* spp.) gradually colonize the soil surface (Weber and others

2016). Biocrust community composition affects ecosystem function, since cyanobacteria, moss, and lichen species have different effects on biogeochemistry, hydrology, soil stability, and energy balance (for example, Bowker and others 2011; Delgado-Baquerizo and others 2015; Torres-Cruz and others 2018). Recent work has demonstrated severe impacts of climate disturbances on biocrust community composition. For instance, Reed and others (2012) showed an increased frequency of small precipitation events (1.2 mm) during summer could drive almost total loss of moss biocrust over a single growing season. Similarly, Ferrenberg and others (2015) demonstrated a shift from late successional moss-lichen biocrust ('Late') to early successional cyanobacterial biocrust ('Early') in response to 6 years of experimental warming—with warming-induced changes similar to impacts seen after more than a decade of repeated human trampling.

These studies provide valuable insight into how climate change may affect biocrust community composition (Reed and others 2012; Ferrenberg and others 2015), net and cumulative CO₂ flux (Darroutzet-Nardi and others 2015; Zhao and others 2016), and climatic sensitivity of different CO₂ fluxes in laboratory (Lange and others 2001; Housman and others 2006; Grote and others 2010) and field settings (Housman and others 2006; Castillo-Monroy and others 2011b; Thomas and others 2011; Escolar and others 2015). Still missing is a conceptual (although see Maestre and others 2013) and quantitative framework for understanding and predicting response to climate change of biocrust-associated CO₂ fluxes relevant at landscape scales (Ferrenberg and others 2017b).

To address this knowledge gap, we evaluated CO₂ fluxes from biocrust mesocosms of different successional states subjected to ambient vs. warmed temperatures over an 84-day period. We used these data to develop a model of biocrust CO₂ fluxes and then compared that model to data from field autochamber measurements of biocrust and soil CO₂ flux responses to experimental warming (+ 2°C). Previous work has established the validity of using biocrust mesocosms as models for representing natural ecosystems (Bowker and others 2014; Maestre and others 2016). The use of mesocosms conferred four advantages: first, the ability to assemble biocrust and soil ecosystems with the desired composition; second, the capacity to accurately assess gross as well as net CO₂ fluxes; third, the ability to carefully control variation in temperature and moisture among treatments, and, finally, reduced effect of antecedent

conditions and differences related to soil chemistry and plant roots. The mesocosms in this study represented three successional states—'Bare' soil, 'Early' successional lightly pigmented cyanobacterial biocrust, and 'Late' successional moss and lichen biocrust—each with distinct traits that suggest differences in how they may respond to increased temperature and changing water availability. We hypothesized: (1) Late successional biocrust communities would have higher rates of gross primary productivity and respiration than Early successional biocrust communities, (2) sensitivity to variation in temperature and moisture would be different among successional states, and (3) the C balance of Late successional biocrusts would be most negatively impacted by warming (that is, increase C losses relative to uptake). These successional states represent a significant fraction of the surface cover of our study region and exhibit potentially predictable inter-stage transitions in response to anthropogenic changes. Thus, developing a predictive understanding of their roles in the ecosystem C cycle would be a major improvement in our understanding of dryland C cycling. To that end, we used data collected from the mesocosm experiment to inform, via Bayesian data-model integration methods, a model of ecosystem CO₂ fluxes in response to temperature and water availability.

METHODS

Biocrust Collection and Experimental Design

Samples were collected from a study site located in a cool desert ecosystem on the Upper Colorado Plateau (36.675N, -109.416W; near Castle Valley, UT) at an elevation of 1310 m above sea level. Mean annual temperature for the surrounding area is 13°C and mean annual precipitation is 269 mm, of which 65% comes in the winter and spring (based on 1981–2010 data; Western Regional Climate Center 2014). Soils are shallow and are classified as sandy loam, calcareous, Rizno series Aridisols. Vegetation is dominated by a native C₃ perennial grass, *Achnatherum hymenoides*; a native C₄ perennial grass, *Hilaria jamesii*; a native C₄ perennial shrub, *Atriplex confertifolia*; and the exotic invasive C₃ grass, *Bromus tectorum*. Biocrust communities are dominated by the cyanobacterium *Microcoleus vaginatus*, the moss *Syntrichia caninervis*, and the cyanolichens *Collema tenax* and *Collema coccophorum*. These species of moss and lichen are common in drylands worldwide and represent

widespread biocrust functional types (Bowker and others 2016).

We assembled mesocosms from biocrusts and soil collected from multiple locations within a single drainage with biocrust communities clearly dominated by either Early or Late successional biocrust communities. Early successional biocrusts were differentiated from bare ground by the presence of visible cyanobacterial filaments. Early and Late biocrust samples were initially wetted to minimize fracturing during removal from underlying soil. A thin metal plate (20 × 30 cm) was then inserted to less than 1 cm below the identified bottom of the biocrust so a large contiguous section could be removed with minimal disturbance. Next, soil was collected to 5 cm depth below where the biocrust sample had been collected. Soils were passed through a 2-mm sieve to remove roots, rocks, and large litter fragments, and collected into a single bucket to homogenize soil collected from below Early and Late biocrusts. We used homogenized soil to avoid the effect of initial differences in soil C cycling between biocrust cover types, and minimize effects resulting from 'home-field' advantage (for example, Strickland and others 2009).

Homogenized soil was added to a depth of 6 cm to a total of 150 plastic pots (8.5 l × 8.5 w × 7 h cm) with holes in the bottom to allow water to freely drain, and with mesh screen to prevent soil from leaking out. To each pot, either Early or Late biocrust was added to completely cover the surface of the soil, or the soil was left bare (Bare soil) ($n = 50$ for each successional treatment). When adding biocrust, we removed soil from the bottom of the biocrust sample that could be easily removed via gentle brushing and scraping—any soil adhering firmly to the biocrust was considered part of the biocrust itself. Mesocosms were assembled in the field and moved into the greenhouse. Initially, mesocosms were watered to water holding capacity for two days to ensure that biocrust recovered from the disturbance associated with mesocosm assembly. Mesocosms were allowed to dry for 8 days prior to the start of the experiment. During the pre-treatment phase, all mesocosms were stored together at greenhouse 'Ambient' temperature.

Mesocosm Conditions and Warming Treatment

Our experiment had six levels: two temperatures and three biocrust successional states, with 25 replicate pots in each. The greenhouse was divided into two rooms with a wall made of two overlapping 6 mil (0.15 mm thickness) translucent poly-

ethylene sheets, creating an Ambient and a Warmed temperature room. The Warmed treatment was implemented using electric and propane heaters (exhausted outside the greenhouse) with thermostatic control, which were adjusted periodically to maintain approximately 7°C warming above ambient air. Air temperatures in both rooms were monitored with four (two per room) Campbell Scientific Model 108 (CS-108) temperature probes shielded by vented, white polyvinyl housing to prevent direct infrared absorption by the probes. Soil temperature was measured using CS-108 thermistors inserted to 5 cm depth in one mesocosm per biocrust level in the Ambient and Warmed treatments. Soil temperatures were on average 5°C higher in the Warmed than Ambient treatment (Supporting Figure S1a and S1b). Across treatments, mean soil temperatures decreased by approximately 25°C from the beginning to end of the experiment due to the seasonal cooling typical in the area's summer to winter transition (Supporting Figure S1a). During the first week of the experiment (September 16–22, 2015) the Warmed soil temperature range (mean [min, max]) was 29.2 [19.0, 45.3]°C, whereas the Ambient range was 26.0 [16.9, 40.1]°C. By the final week (December 2–8, 2015), the Warmed soil temperature range was 9.0 [1.5, 31.4]°C, while the Ambient range was 3.5 [– 2.0, 18.7]°C. The maximum soil T measured in this study (50.3°C) was lower than the maximum measured at the field site (57.2°C) using the same type of soil temperature probe inserted to the same depth.

We subjected mesocosms to a pulse-watering regime. Deionized water (120 ml) was added to each mesocosm once per week, after which mesocosms were allowed to dry. Watering was done in four 30 ml aliquots over the course of 2 h in the morning. Added water was equivalent to a 16.6 mm rain event, which would be a moderately large event for our study region and resulted in the equivalent of 74% of annual average precipitation in an 84-day period. Because mesocosms have substantially more surface area for a given volume and drain more freely than soil in the field, the soils dried rapidly (see Figure 1) and underwent the full range of moisture conditions experienced in the field. The watering regime was designed to reduce water pooling at the biocrust surface, or being lost via runoff, and to allow substantial infiltration. CO₂ flux measurements were started 1 h after watering ended to avoid the initial CO₂ pulse associated with wetting and to allow the wetted surface sufficient time to drain and be aerated. It is unlikely that a substantial diffusion barrier associated with water films at the

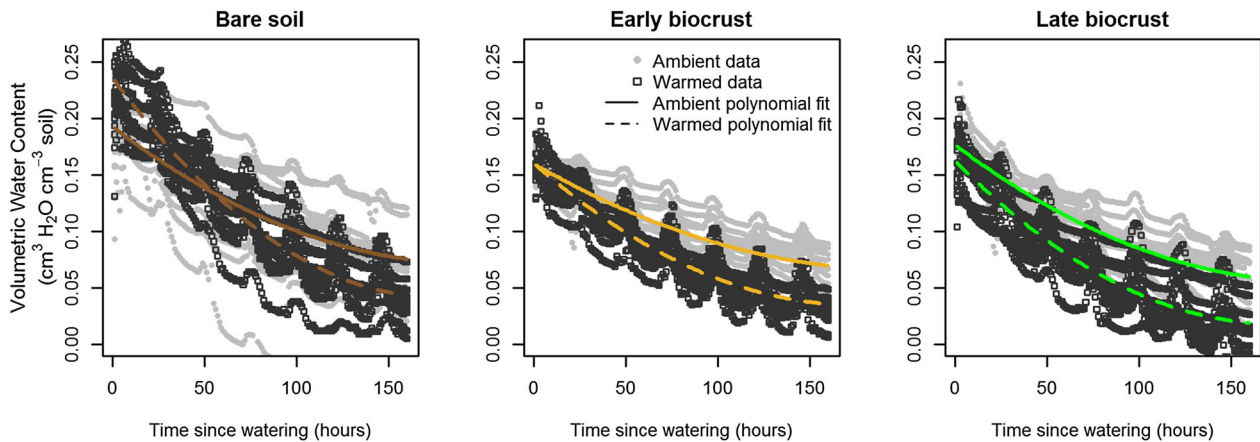


Figure 1. Volumetric water content of the soil profile across all wet–dry cycles for each biocrust successional state in the study, where the x -axis is time since watering. Lines for each biocrust state and treatment (ambient vs. warmed) were fitted via polynomial regression using R statistical software, and the slopes of the lines were compared using ANCOVA. The fit of the polynomial regression was as follows: Bare-Warmed ($r^2 = 0.857$, $p < 0.001$), Bare-Ambient ($r^2 = 0.485$, $p < 0.001$), Early-Warmed ($r^2 = 0.864$, $p < 0.001$), Early-Ambient ($r^2 = 0.723$, $p < 0.001$), Late-Warmed ($r^2 = 0.804$, $p < 0.001$), Late-Ambient ($r^2 = 0.775$, $p < 0.001$). Ambient data are shown as *filled gray circles* and Warmed data are shown as *unfilled black squares*. The rate of soil drying was higher in the Warm treatment relative to ambient across all successional states ($p < 0.001$).

surface was present when we started the measurements, but we cannot rule out that possibility. Soil volumetric water content (VWC) was measured using Decagon EC-5 probes between 0 and 5 cm in one mesocosm per biocrust level in the Ambient and Warmed treatment. Time series of soil VWC are presented in Supporting Figure S2.

Photosynthetically active radiation (PAR) was monitored in each room by two Apogee Instruments Quantum Sensors SQ-215 (one per room) placed centrally among the mesocosms. We changed mesocosm position in relation to changes in sun angle throughout the experiment to minimize light difference between rooms. PAR, VWC, and temperature were measured every 10 min and accumulated into hourly averages.

Measurement of CO₂ Fluxes

On 30 measurement dates between September 15, 2015, and December 9, 2015, we measured CO₂ fluxes in a transparent chamber to measure net soil exchange (NSE), which includes photosynthesis by biocrust, and respiration by both biocrust and heterotrophs in the soil beneath the biocrust, then placed mesocosms in a dark box for between 30 and 45 min to shut off CO₂ assimilation before measuring CO₂ fluxes in an opaque chamber to measure respiration (R). Measurements were made each week within 4 h of watering ('Wet' phase), 24 h after watering ('Moist' phase) and 6 days after watering ('Dry' phase) using a LI-8100A Automated

Soil Gas Flux System (Li-Cor Inc., Lincoln, NE, USA). CO₂ fluxes were calculated using Li-Cor File Viewer software by either the linear or exponential fit to the water-corrected CO₂ concentration change over a 2.5-min period following a 30-s dead band. Measurements were only conducted when ambient CO₂ concentrations in the greenhouse were below 450 ppm. CO₂ concentrations in excess of 450 ppm occurred as a result of either smoke from nearby fires (which was a region-wide issue and would also have been experienced by biocrust in situ), or when people worked in the greenhouse without turning on ventilation, which was addressed by improving ventilation. On each date, NSE and R were measured in 5 replicate mesocosm pots within each of six treatment levels ($n = 30$ total per date). Measurement order was assigned randomly, and fluxes were measured in blocks of 10 so that measurements in transparent and opaque chambers could be paired closely in time. Issues with power supply, smoke from nearby fires, or mistaken protocol resulted in partial data loss, such that 80 out of 900 planned measurements were not made or were discarded; nonetheless, the resulting data set consisted of 820 paired measurements (that is, 1640 individual CO₂ flux measurements) of NSE and R. Respiration in Bare soil was equal to heterotrophic soil respiration (R_s) and in the Early and Late biocrusts was equal to R_s plus biocrust respiration (R_c). Gross primary productivity (GPP) was calculated as the difference between NSE and R. We use the convention that fluxes into the atmosphere are positive, so that R has

a positive sign, and GPP has a negative sign, while NSE can have either positive or negative values.

Data Analysis and Modeling

Data analysis was conducted in the context of a model of biocrust and soil CO₂ fluxes (equations 1–10), where R is modeled as a function of soil volumetric water content (VWC) and temperature (T), with parameters varying by biocrust stage (that is, Late, Early, Bare), and GPP is modeled as a function of VWC, T , and PAR.

For $i = 820$ individual measurements of CO₂ fluxes for R and NSE (that is, 1640 total measurements), GPP was calculated as the difference between R and NSE (equation 1).

$$\text{NSE}_i = R_i + \text{GPP}_i \quad (1)$$

We modeled the mean flux of each treatment level ($j = 6$ combinations of three biocrust levels (b) and two climate levels (c)) on each date ($k = 30$), assuming data were normally distributed around the latent ‘true’ mean, denoted by the symbol μR and μGPP (equations 2 and 3).

$$R_i \sim \text{normal}(\mu R_{j,k}, \sigma_R) \quad (2)$$

$$\text{GPP}_i \sim \text{normal}(\mu \text{GPP}_{j,k}, \sigma_{\text{GPP}}) \quad (3)$$

We then modeled the latent mean fluxes as functions of climate parameters. μR was modeled in equation (4) by multiplying a basal respiration rate (R_{base}), a Lloyd and Taylor temperature response function (Lloyd and Taylor 1994) (f_{rt} , equation 5), and a Gompertz soil moisture response function (Janssens and others 2001) (f_{rv} , equation 6), as described in detail in Tucker and Reed (2016) (equations 4, 5, 6).

$$\mu R_{j,k} = R_{\text{base},j} \times f_{\text{rt}}(T_{j,k}) \times f_{\text{rv}}(\text{VWC}_{j,k}) \quad (4)$$

$$\begin{aligned} f_{\text{rt}}(T_{j,k}) \\ = \exp\left(E_{o,b(j)} \times \left(\frac{1}{293.15 - T_{o,b(j)}} - \frac{1}{T_{j,k} - T_{o,b(j)}}\right)\right) \end{aligned} \quad (5)$$

$$\begin{aligned} f_{\text{rv}}(\text{VWC}_{j,k}) \\ = \exp\left(-\exp\left(\alpha_{r,b(j)} - \beta_{r,b(j)} \times \text{VWC}_{j,k} \times 100\right)\right) \end{aligned} \quad (6)$$

μGPP was modeled in equation (7) by multiplying a temperature response function indicating a maximum value at T_{opt} and declining to 0 at T_{min} and T_{max} (Raich and others 1991) (f_{gt} , equation 8),

a Gompertz soil moisture response function (f_{gv} , equation 9), and a Michaelis–Menten function for PAR response (f_{gp} , equation 10), with parameters coarsely derived from Lange and others (2003), Marschall and Proctor (2004).

$$\mu \text{GPP}_{j,k} = \text{GPP}_{\text{base}} \times f_{\text{gt}}(T) \times f_{\text{gv}}(\text{VWC}_{j,k}) \times f_{\text{gp}}(\text{PAR}) \quad (7)$$

$$\begin{aligned} f_{\text{gt}}(T_{j,k}) \\ = \frac{(T_{j,k} - T_{\text{min},b(j)}) \times (T_{j,k} - T_{\text{max},b(j)})}{(T_{j,k} - T_{\text{min},b(j)}) \times (T_{j,k} - T_{\text{max},bv(j)}) - (T_{j,k} - T_{\text{opt},b(j)})^2} \end{aligned} \quad (8)$$

$$\begin{aligned} f_{\text{gv}}(\text{VWC}_{j,k}) \\ = \exp\left(-\exp\left(\alpha_{n,b(j)} - \beta_{n,b(j)} \times \text{VWC}_{j,k} \times 100\right)\right) \end{aligned} \quad (9)$$

Because we lack data to precisely model PAR responses, our PAR parameterization dictates substantial photosynthesis at low light levels (for example, $< 500 \mu\text{mol m}^{-2} \text{s}^{-1}$), and light saturation at moderate levels (for example, $< 1000 \mu\text{mol m}^{-2} \text{s}^{-1}$), which is consistent with some available studies on light response curves of photosynthesis in biocrust organisms (Green and Proctor 2016).

$$f_{\text{gp}}(\text{PAR}) = \frac{\text{PAR}}{100 + \text{PAR}} \quad (10)$$

A crucial feature of this analysis is that model parameter values were estimated using Bayesian data–model integration (Ogle and Barber 2008), based on our mesocosm CO₂ flux data, and on soil temperature, soil moisture, and PAR conditions in the greenhouse. Thus, parameter estimates account for uncertainty in the data as well as the accuracy of the model. Parameters in the model were estimated using Bayesian statistical methods implemented using the STAN software package (Stan Development Team. 2015. *Stan Modeling Language Users Guide and Reference Manual, version 2.7.0.*) on the R (v 3.2) statistical platform. Four Markov chain Monte Carlo (MCMC) chains were run for 20,000 iterations, and the first 10,000 were discarded as a burn-in period. Model convergence was evaluated using the built-in \hat{R} metric, where $\hat{R} = 1$ at convergence. The model and data are provided as Supporting Information S5–S9. For details of Bayesian data analysis, refer to Gelman and others (2004).

To estimate cumulative NSE, GPP, and R over the duration of the experiment, flux rates were mod-

eled hourly based on measured T, VWC, and PAR measurements; then, modeled fluxes were summed. Uncertainty in the data model was propagated through the flux predictions (both the hourly and cumulative fluxes) using Bayesian methods. To evaluate how well the model-based on mesocosm data-captured patterns CO₂ exchange observed in the field, we used our model to simulate Late biocrust NSE using 22 months (January 2006–October 2007) of soil temperature, soil moisture, and PAR data from Late biocrust patches occurring within 500 m of the biocrust mesocosm collection location. NSE of these Late biocrust patches was independently measured for that interval in the field using autochambers, offering an unparalleled opportunity to confront our model with field data [autochamber methods and data are described in detail in Darrouzet-Nardi and others (2015)]. All post-processing of model results was done in R (v 3.2) statistical software.

RESULTS

Soil Temperature and Moisture

The average soil temperature was 5.2, 4.8, and 5.0°C higher in the Warmed than Ambient treatment for Bare soil, Early, and Late biocrust, respectively ($p < 0.001$ for each, Supporting Figure S1a and b), and seasonal patterns varied as described in the Methods. Warmer temperatures resulted in more rapid soil drying (Figure 1, $p < 0.001$ for polynomial regression). There were 12.8, 32.7, and 31.9% fewer hours with soil moisture above $0.08 \text{ cm}^3 \text{ H}_2\text{O cm}^{-3}$ soil [a threshold below which soil respiration decreased dramatically in a study from the same site (Tucker and Reed 2016)] in the Warmed treatment compared with Ambient for Bare soil, Early, and Late biocrust, respectively ($p < 0.001$). In general, within 4 h after watering ('Wet' phase) soil moisture was equal in Warmed and Ambient treatments in Early and Late biocrust, and slightly higher in the Warmed vs. Ambient treatment in Bare soil. VWC was consistently greater in the Ambient treatment 1 day after watering ('Moist' phase) and 6 days after watering ('Dry' phase) (Figure 1, Supporting Figure S2). Some differences in soil moisture between Warmed and Ambient treatments may be due to a temperature dependence of the soil moisture probes, where a 10°C warming might result in approximately $0.02 \text{ cm}^3 \text{ cm}^{-3}$ overestimation of soil water content (Kizito and others 2008).

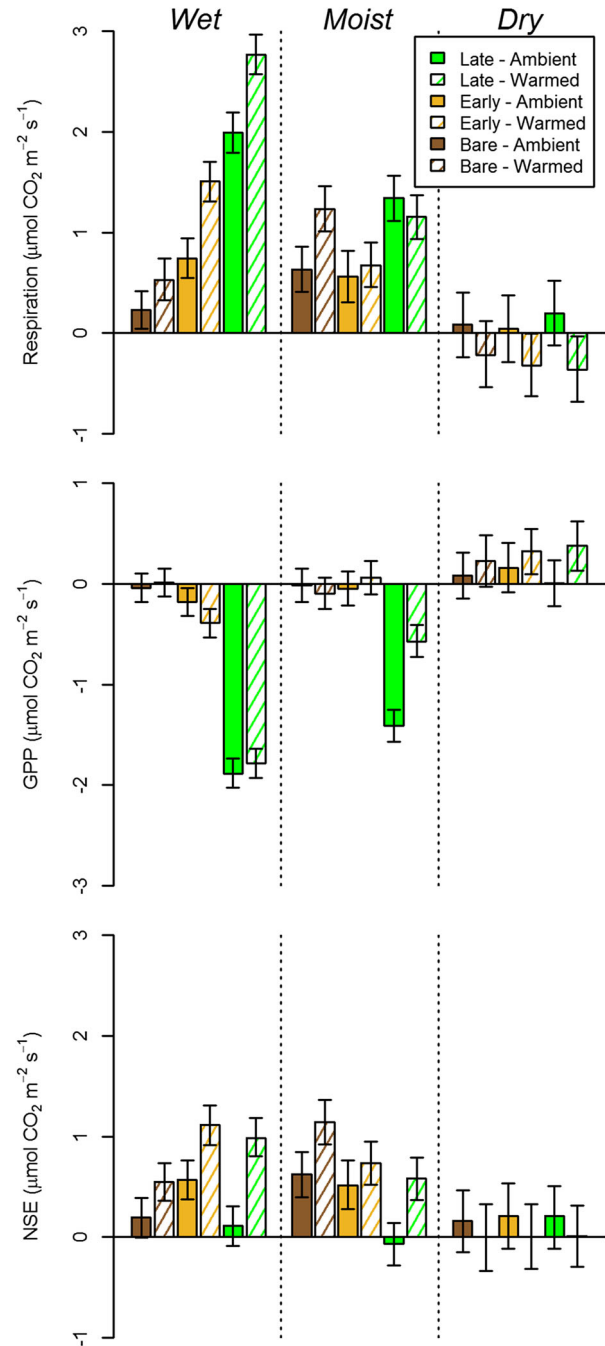


Figure 2. The mean of measured respiration (*top*), gross primary production (GPP; *middle*), and net soil CO₂ exchange (NSE; *bottom*) across all wet (*left*), moist (*middle*), and dry (*right*) phases. Rates are shown for bare soil (bare; *brown*), early successional biocrusts (early; *orange*), and late successional biocrusts (late; *green*) in both ambient (*filled bars*) and warmed (*striped bars*) conditions. *Error bars* represent Bayesian 95% credible intervals: where the error bars of one group do not overlap the mean of another group, the differences are significant.

Measured CO₂ Fluxes

Both R and GPP were larger in Late than in Early biocrust, and lowest in Bare soil (Figure 2 and Supporting Figure S3). Respiration decreased in all treatments over the experiment (Supporting Figure S3) and was higher at warmer temperatures immediately after watering ('Wet' phase), before any observable effect of warming on soil moisture occurred (Figure 2 'Wet'). During the 'Moist' phase, 1 day after watering, R was equal between Warmed and Ambient treatments in the Late and Early biocrust, but higher in the Warmed than Ambient treatment in Bare soil. During the 'Dry' phase, 6 days after watering, R was low, but higher in Ambient than Warmed treatments (Figure 2 'Dry'). Gross primary productivity did not show a clear seasonal trend in either Early or Late biocrust (Supporting Figure S3) and was only weakly related to temperature during the 'Wet' phase (Figure 2 'Wet'). As soils dried, the 'Moist' phase GPP of Late biocrust was lower in the Warmed than Ambient treatment (Figure 2 'Moist'). During the 'Dry' phase, GPP was extremely low, and lower in the Warmed than Ambient treatments. Net soil CO₂ exchange, which is the sum of R and GPP, increased with temperature during the 'Wet' and 'Moist' phase (that is, warming caused a net loss of C from the bare soil and both biocrust states). NSE was very low during the 'Dry' phase. Average NSE during the 'Wet' and 'Moist' phase was neutral or negative (that is, overall, C was gained by the soil and biocrust) in Late biocrust at Ambient temperature, but positive (that is, overall, C was lost by the

soil and biocrust) in all other treatments (Figure 2). As seasonal temperatures declined, R decreased, but GPP in Late biocrust did not, such that net C uptake (that is, negative NSE) occurred more frequently later in the experiment (Supporting Figure S3).

Modeled CO₂ Fluxes

In general, the model fit the data well (Figure 3), although the fit was better for the R component than the GPP component of NSE ($r^2 = 0.861$, 0.794, and 0.761, for R, GPP, and NSE, respectively). Parameter values (mean and 95% posterior credible intervals) are presented in Table 1. After 84 days under greenhouse treatments, modeled cumulative R was higher in the Ambient than Warmed treatment in Late biocrust, but was higher in the Warmed than Ambient treatment in Early biocrust and Bare soil (Figure 4A). Modeled cumulative GPP was much higher in the Ambient than Warmed treatment in Late biocrust, and equal across Warmed and Ambient treatments in Early biocrust (Figure 4B). For the Early biocrust, cumulative GPP was only 9.97% of the Late biocrust values (Figure 4B). Cumulative NSE was positive (that is, overall, C was lost from the ecosystem) in all treatments and was significantly higher in the Warmed treatment in Early biocrust and Bare soil, although not in Late biocrust (Figure 4C).

Temporal patterns of cumulative CO₂ fluxes are presented in Figure 5. Both R (Figure 5A–C) and GPP (Figure 5D–E) exhibit pulse dynamics, where

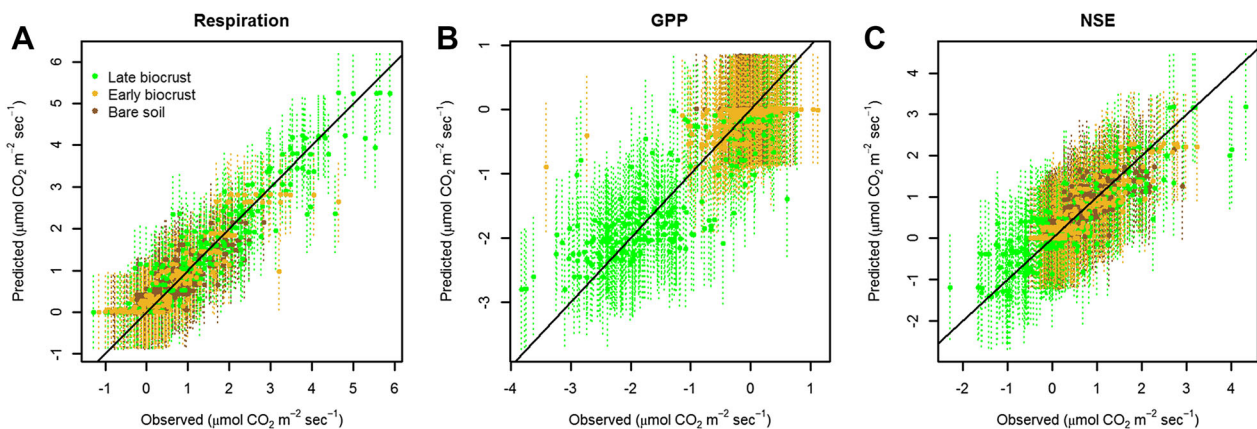


Figure 3. Predicted versus observed fluxes of respiration (R; *left*), gross primary production (GPP; *middle*), and net soil CO₂ exchange (NSE; *right*) comparing data–model results to measured data. Dotted vertical lines represent Bayesian 95% credible intervals for each predicted flux. Each panel's solid line is the one-to-one line indicating perfect correlation between predicted and observed values. Data shown are for bare soil (bare; brown), early successional biocrusts (early; orange), and late successional biocrusts (late; green). All predicted versus observed fluxes fell along the one-to-one line and the model fit the data well.

Table 1. Posterior Mean and 95% Credible Intervals for All Parameters in Equations (4–10)

Parameter (units)	Eqn.	Units	Mean	2.50%	97.50%	\hat{R}
E_o Bare soil	5	°K	316.816	278.742	355.558	1.00
E_o Late biocrust	5	°K	311.566	273.648	348.99	1.00
E_o Early biocrust	5	°K	312.05	273.597	350.754	1.00
T_o Bare soil	5	°K	255.125	249.764	260.237	1.00
T_o Late biocrust	5	°K	228.222	220.005	235.51	1.00
T_o Early biocrust	5	°K	237.042	225.087	246.666	1.00
R_{base} Bare soil	4	$\mu\text{mol CO}_2 \text{ m}^{-2} \text{ s}^{-1}$	0.157	0.097	0.224	1.00
R_{base} Late biocrust	4	$\mu\text{mol CO}_2 \text{ m}^{-2} \text{ s}^{-1}$	3.715	2.34	5.7	1.00
R_{base} Early biocrust	4	$\mu\text{mol CO}_2 \text{ m}^{-2} \text{ s}^{-1}$	4.662	2.647	6.653	1.00
α_r Bare soil	6	Unitless	60.383	14.942	97.955	1.00
α_r Late biocrust	6	Unitless	2.889	2.285	3.977	1.00
α_r Early biocrust	6	Unitless	2.819	2.397	3.454	1.00
β_r Bare soil	6	$\text{cm}^3 \text{ H}_2\text{O cm}^{-3} \text{ soil}$	5.53	1.391	9.319	1.00
β_r Late biocrust	6	$\text{cm}^3 \text{ H}_2\text{O cm}^{-3} \text{ soil}$	0.191	0.128	0.297	1.00
β_r Early biocrust	6	$\text{cm}^3 \text{ H}_2\text{O cm}^{-3} \text{ soil}$	0.135	0.1	0.192	1.00
GPP_{base} Late biocrust	7	$\mu\text{mol CO}_2 \text{ m}^{-2} \text{ s}^{-1}$	3.954	3.219	5.083	1.00
GPP_{base} Early biocrust	7	$\mu\text{mol CO}_2 \text{ m}^{-2} \text{ s}^{-1}$	22.09	0.667	92.202	1.00
α_g Late biocrust	9	Unitless	10.607	6.598	16.643	1.00
α_g Early biocrust	9	Unitless	17.394	3.056	90.351	1.00
β_g Late biocrust	9	$\text{cm}^3 \text{ H}_2\text{O cm}^{-3} \text{ soil}$	0.785	0.485	1.231	1.00
β_g Early biocrust	9	$\text{cm}^3 \text{ H}_2\text{O cm}^{-3} \text{ soil}$	1.071	0.09	5.879	1.00
T_{min} Late biocrust	8	°C	− 22.299	− 47.989	− 5.424	1.00
T_{min} Early biocrust	8	°C	− 27.033	− 48.802	− 6.102	1.00
T_{max} Late biocrust	8	°C	53.004	38.815	84.704	1.00
T_{max} Early biocrust	8	°C	63.172	35.817	98.059	1.00
T_{opt} Late biocrust	8	°C	13.718	0.906	23.354	1.00
T_{opt} Early biocrust	8	°C	19.908	0.925	43.62	1.00

Parameter values are not presented for the gross primary production (GPP) functions for the Bare soil treatment, because GPP was not observed or expected: the model correctly estimated zero GPP in Bare soil, such that the parameter values in the component functions were completely unconstrained and took on a wide range of meaningless values. \hat{R} is the potential scale reduction factor on split chains, and when MCMC chains have converged $\hat{R} = 1$. Please note that some temperature units are Celsius and others are Kelvin, which is done for consistency with other studies using these same functions.

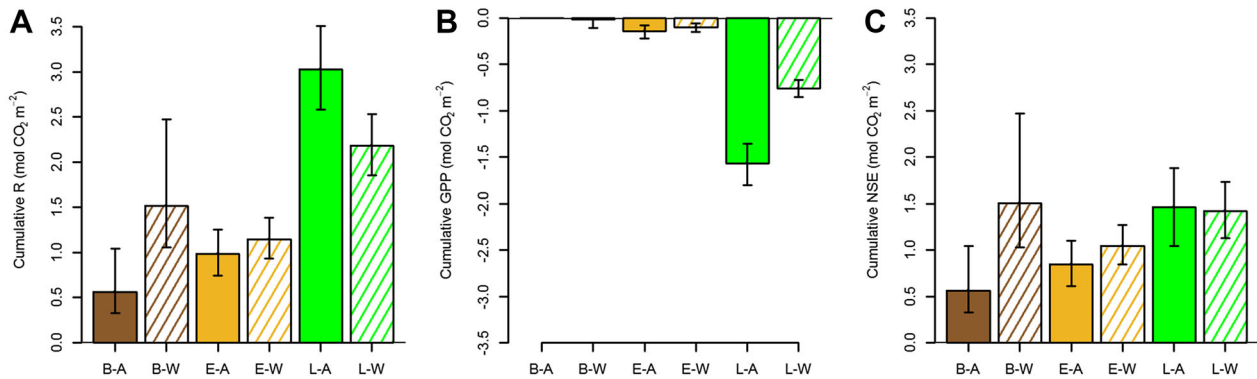


Figure 4. Final cumulative respiration (R) (A), gross primary production (GPP) (B), and net soil CO₂ exchange (NSE) (C) as estimated from the data model, with error bars representing Bayesian 95% credible intervals. Where the error bars of one group do not overlap the mean of another, the difference is significant. X-axis labels correspond to biocrust successional level and temperature treatment (for example, B–W means Bare soil Warmed, L–A means Late Ambient). Values shown are from Bare soil (B; brown), Early successional biocrusts (E; orange), and Late successional biocrusts (L; green).

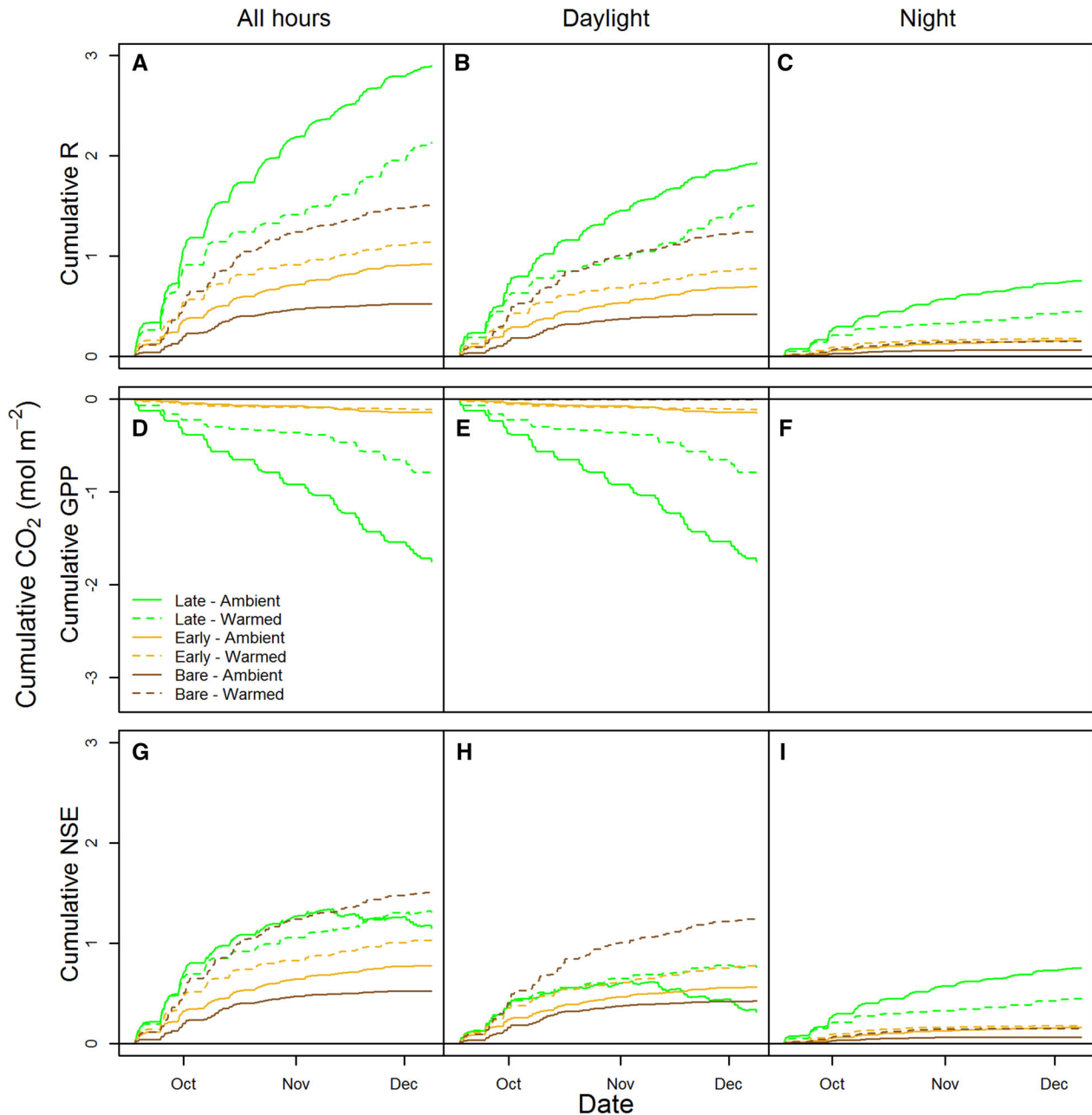


Figure 5. Cumulative sum of respiration (R; *top row*), gross primary production (GPP; *middle row*), and net soil CO₂ exchange (NSE; *bottom row*) from the data model. The left column shows the cumulative flux across all hours, the middle column shows the cumulative flux when photosynthetically active radiation is above $1 \mu\text{mol photon m}^{-2} \text{s}^{-1}$ (that is, daylight hours), and the right column shows cumulative fluxes in the dark ($\text{PAR} \leq 1 \mu\text{mol photon m}^{-2} \text{s}^{-1}$). Green lines represent Late successional biocrusted soil, orange lines represent Early successional biocrusted soil, and brown lines represent Bare soil. Solid lines are for Ambient treatment mesocosms and dashed lines are for Warmed treatment mesocosms.

nearly all of the cumulative fluxes occurred in the brief interval following water events, and plateaued during dry periods. In Late biocrust, cumulative GPP in the Ambient treatment increased steadily over the experiment, yet in the Warmed treatment GPP showed a noticeable uptick in mid-November.

The model predicts low R at night (Figure 5C), corresponding to lower temperatures, and no GPP at night (Figure 5F.), because night is defined as the period when $\text{PAR} < 1 \mu\text{mol photons m}^{-2} \text{s}^{-1}$. For most of the experiment, Late biocrust NSE was higher in the Ambient treatment, in mid-Novem-

ber, as seasonal temperatures cooled, Late biocrust in the Ambient treatment began to accumulate CO₂ during daylight hours (Figure 5H), such that daylight NSE was lower in the Ambient than Warmed treatment by the end of the experiment. Cumulative NSE of Late biocrust at night was higher in the Ambient treatment throughout the experiment (Figure 5I), such that nighttime efflux of CO₂ partly balanced out daylight gain by Late biocrust (Figure 5H).

The model-predicted instantaneous NSE increased with temperature in Bare soil and was low below approximately 20°C (Figure 6A). Predicted NSE was higher in Early biocrust than Bare soil between about 15 and 35°C, whereas between 0 and 15°C there was net uptake of CO₂ in Early biocrust (Figure 6A). Late biocrust showed lowest NSE (that is, highest uptake of CO₂) at low temperatures, between 0 and 25°C with an optimum at 10°C, but also exhibited higher CO₂ efflux at lower temperatures (Figure 6A). In general, NSE was low below VWC ≈ 0.08 (Figure 6B). NSE was always positive in Bare soil above that threshold and was not related to VWC above or below the 0.08 breakpoint, suggesting a critical value of soil moisture for Bare soil R in this system (Figure 6B). Biocrust only exhibited uptake in a narrow window of soil moisture: for Early biocrust this window was between VWC = 0.15 and 0.18, and for Late biocrust between VWC = 0.12 and 0.20 (Figure 6B).

We compared simulated and measured Late biocrust NSE from autochambers operating continuously at the field site (Figure 8C) and found that during most of that period rates of NSE were quite similar, although maximum simulated fluxes

(both positive and negative) were greater in the modeled data. The model captured most major C uptake and loss events, and the seasonality of C uptake and loss showed the same patterns. However, our simulations markedly underestimated CO₂ efflux during hot-dry periods (black boxes in Figure 8), leading to a relatively poor model fit to field data when compared across all time points (Supporting Figure S5)

DISCUSSION

Climate change and physical disturbance have the potential to substantially alter the successional state of biocrust on the Colorado Plateau (for example, Belnap and others 2004; Reed and others 2012; Pointing and Belnap, 2014; Ferrenberg and others 2015; Reed and others 2016). In this study, we demonstrate that the climatic sensitivity of ecosystem CO₂ exchange differed among biocrust successional states (Figure 7). In particular, Late successional biocrust exhibited much higher instantaneous and cumulative rates of gross primary production and respiration than Early successional biocrust or Bare soil, but also were more inhibited by warming.

In general, elevated temperature drove more rapid drying of biocrusts and soil (Figure 7A). Because of this temperature x moisture interaction, the net effect of warming (Figure 7B) was increased R_s (soil respiration), increased or decreased R_c (biocrust respiration) depending on biocrust successional state, and decreased biocrust GPP. All soil and biocrust CO₂ fluxes were positively related to soil

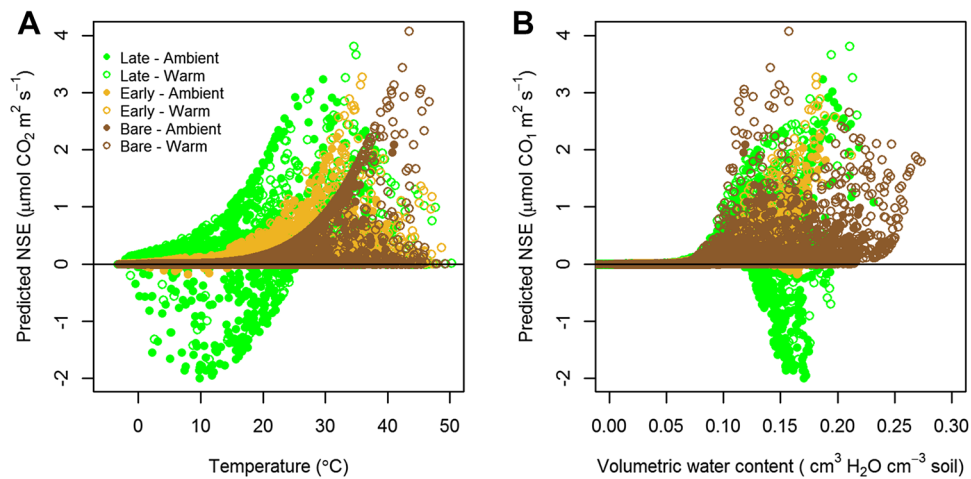


Figure 6. Modeled net soil exchange (NSE; R + GPP) of different biocrust successional states as a function of soil (A) temperature and (B) volumetric water content. Green circles represent late successional biocrusted soil, orange circles represent early successional biocrusted soil, and brown circles represent bare soil. Filled circles are ambient treatment mesocosm data, and unfilled circles are warmed treatment mesocosm data.

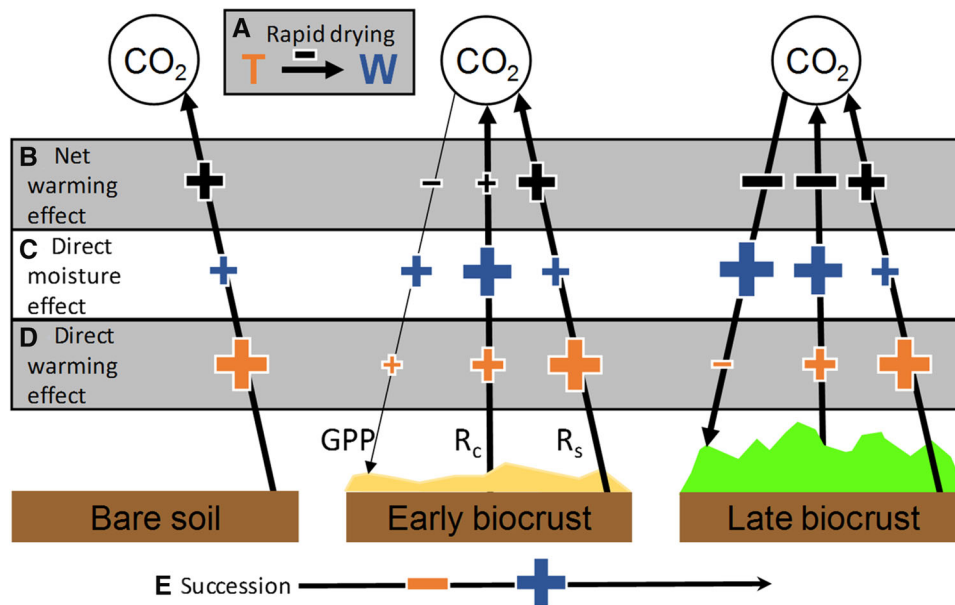


Figure 7. Conceptual model of the temperature (T , orange symbols) and moisture (W , blue symbols) controls over biocrust soil CO₂ exchange with the atmosphere. Plus signs (+) indicate a stimulatory effect of a control on a given flux of CO₂ to or from the atmosphere, and a minus sign (–) indicates a reduction of a CO₂ flux. Larger symbols indicate larger effects. Three biocrust successional states are represented (Bare, Early, and Late), and atmospheric CO₂ is represented by CO₂ inside the circles at the top of the figure. The direction of the flux is indicated by (→) and the width of the arrows approximately depicts the flux’s relative magnitude. **A** Temperature x moisture interaction, **B** net effect of warming (including indirect effects of drying) on CO₂ fluxes, **C** direct effect of soil water availability on CO₂ fluxes **D** direct effect of warming on CO₂ fluxes **E** effect of warming and soil water availability on biocrust succession. It is important to note that increased frequency of small precipitation events during the warm season can also cause a net loss of Late successional biocrust (Reed and others 2012). We use the temperature and moisture responses of Bare soil to infer R_s across mesocosms.

moisture availability, thus drying decreased fluxes (Figure 7C), while elevated temperatures directly (that is, excluding the effect of drying) increased all CO₂ fluxes with the exception of Late biocrust GPP, which was weakly inhibited by warming (Figure 7D). The dominant effect of elevated temperature was thus the indirect negative effect mediated through accelerated drying. These facts take on added importance because climate warming may drive loss of Late successional biocrust and replacement by Early successional biocrust (for example, Maestre and others 2012a; Maestre and others 2013; Ferrenberg and others 2015).

Thus, we can expect in the short-term (that is, sub-annual scale) warming and drying will reduce ecosystem C cycling rates by reducing Late successional biocrust activity, and in the longer term (years to decades), reduce ecosystem C cycling by causing the replacement of Late biocrust with Early biocrust or Bare soil. The long-term impact is likely to be reduced C uptake and a net loss of C from the ecosystem. Biocrusts are important components of the C cycle at our study site, and potentially at myriad dryland sites worldwide (Elbert and others

2012; Sancho and others 2016). Based on recent work demonstrating the likely importance of drylands in regulating the C cycle globally (Poulter and others 2014; Ahlström and others 2015), and considered in conjunction with the often overlooked importance of biocrust C cycling (Elbert and others 2012; Sancho and others 2016), we suggest that the framework presented in Figure 7 (and the related model functions) merits consideration as a component of ecosystem and Earth system models of the terrestrial C cycle.

Biocrust Succession in Drylands Interacts with Climate, Disturbance and the C Cycle

After severe disturbance, biocrust succession generally progresses through stages similar across many drylands (Weber and others 2016). Bare soil is colonized by lightly pigmented, early successional cyanobacteria, which stabilize the soil surface allowing for subsequent establishment of moss and/or lichen. Conversely, moss and lichen replacement by cyanobacterial biocrust occurs in

response to physical trampling, and, at least in some cases, in response to warming and altered precipitation (Ferrenberg and others 2015). Our results provide both a mechanistic framework for interpreting the causes of the transition from Late moss-lichen to Early cyanobacterial biocrust, and insight into consequences of such a transition for the ecosystem C cycle. We demonstrate that C uptake by biocrust is negatively affected by warming in Late biocrust but not in Early biocrust. Thus, a transition from Late to Early biocrust under warming may be a function of reduced C uptake of mosses and lichens leading to C starvation and gradual colonization of the newly available soil surface by cyanobacteria more tolerant of hotter conditions. Because warming could cause a transition of Late to Early biocrust, and because Early biocrusts fix much less C from the atmosphere than Late biocrust (Figure 2), we expect such a successional regression to be associated with significantly lower rates of C uptake in biocrusted drylands. Finally, stimulation of R by warming in Bare soil suggests a net loss of sub-crust soil C in response to warming, independent of biocrust successional stages. This suggestion is supported by the observation that, at the global scale, soil C declines with increasing aridity (Delgado-Baquerizo and others 2013).

These climatic influences on the C flux of different biocrust successional states likely extend to ecosystem C balance as well. At our study site, maximum soil respiration rates from biocrusted interspaces were similar to maximum soil respiration rates beneath the canopy of *Atriplex confertifolia* (3.2 versus 4.4 $\mu\text{mol CO}_2 \text{ m}^{-2} \text{ s}^{-1}$), suggesting large efflux of CO₂ from biocrusted soils (Tucker and Reed 2016). The maximum rates of biocrust C fixation per unit photosynthetic area are also on the same order of magnitude to maximum rates achieved by vascular plants at this site (for example, 3.8 $\mu\text{mol m}^{-2} \text{ s}^{-1}$ for moss-dominated biocrust (this study) versus leaf level photosynthetic rates of about 11-20 $\mu\text{mol m}^{-2} \text{ s}^{-1}$ for the three dominant plant species at this site (Wertin and others 2015)). Considering that biocrust surface area can exceed leaf surface area, and that biocrusts can uptake C any time of year, unlike vascular plants that undergo multi-month senescent states (for example, under snow photosynthesis is notable at this site; Darrouzet-Nardi and others 2015), biocrust photosynthesis and respiration may be the largest CO₂ fluxes in some ecosystems. For example, Castillo-Monroy and others (2011b) demonstrated that soil respiration from biocrusted interspaces was the dominant CO₂ efflux in a dryland ecosystem similar

to the Colorado Plateau site described here, largely because biocrusted interspaces were the dominant land cover type. Thus, although a handful of studies suggest that biocrusts could be significant components of dryland C uptake, storage, and release (for example, Sancho and others 2016), our quantification and contextualization of these rates, and our understanding of the controls over them, has remained notably poor. In this context, the data presented here represent an important look into these fluxes, how they vary over fine temporal scales and across biocrust successional states, and advance our understanding of their sensitivity to alterations in temperature and moisture.

Late Successional Biocrust CO₂ Fluxes

Rates of C cycling in Late biocrust were higher than in Early biocrust or Bare soil. Both R and GPP of Late biocrust were highly sensitive to soil moisture: high fluxes during the Wet phase diminished rapidly as soils dried. Within hours of wetting, respiration (R) in Late biocrust was enhanced by warming, but this stimulation transitioned to inhibition as biocrust and soils dried more rapidly under the Warmed treatment. This result agrees with a field soil respiration study at a nearby site, which suggested stronger indirect controls of temperature via drying relative to direct negative temperature control over soil CO₂ efflux (Tucker and Reed 2016). Late biocrust GPP was also inhibited by warming due to accelerated soil drying; there was only a small negative direct effect of warming on Late biocrust GPP. This result agrees with findings by Li and others (2012) that biocrust photosynthesis was determined by water content rather than either PAR or temperature. In addition, Late biocrust showed the largest imbalance between instantaneous daytime CO₂ uptake and loss in response to warming. Specifically, under the Ambient temperature treatment, NSE of the biocrust and subsurface soil was neutral or only slightly positive, whereas under Warmed conditions the instantaneous daytime balance of CO₂ showed a large net loss to the atmosphere.

Cumulative NSE as estimated from our data model showed a different pattern than implied by measured instantaneous fluxes (compare Figures 2, 6, 7 NSE). For the first two months of the experiment, NSE of Late biocrust was lower under Warmed conditions. This pattern was largely driven by reduction of nighttime R under the Warmed treatment (as a result of drying), which more than balanced the reduction of daytime GPP under the Warmed treatment during warmer seasonal con-

ditions earlier in the experiment. As seasonal temperatures cooled (Supporting Figure S1a), this pattern reversed, and the Late biocrust under Ambient temperatures began to uptake enough C during daylight to more than offset nighttime respiratory loss, which is similar to patterns observed in a semiarid shrubland in Israel (Wilske and others 2008). Thus, under Ambient conditions, Late biocrust showed net C uptake during the cool season, indicating growth and recovery from heat stress during the warm season, supporting previous work from the same study site (Darrouzet-Nardi and others 2015; Ferrenberg and others 2015). By the end of the experiment, the trajectory was toward increasing C uptake in Ambient conditions, but increasing C loss under Warmed conditions. Climate projections for our region suggest a reduction in the duration of the cool-wet winter period (Klos and others 2014), which considering our results suggests a reduction in C uptake by Late biocrusts.

Early Successional Biocrust CO₂ Fluxes

Rates of C cycling in Early successional biocrust were overall lower than in Late biocrust. In Early biocrust, both R and GPP were stimulated by Warming under wet conditions, although the low rates of C uptake make it difficult to evaluate the exact response of GPP to environmental conditions. These differences disappeared 24 h after wetting, at which point C uptake was no longer measurable. Respiration of Early biocrust mesocosms declined substantially in the Warmed treatment between the Wet and Moist phase, but not in the Ambient treatment, suggesting that the increased rate of soil drying was a critical factor. This interpretation is further supported by the fact that R was lower in the Warmed treatment during the Dry phase. Interestingly, there were no differences in the modeled cumulative R, GPP, or NSE between Ambient and Warmed treatments in the Early biocrust. This result may reflect a tradeoff between stimulation of GPP in the Warmed treatment during the Wet phase, and inhibition during the Dry phase. One interpretation is that the dominant Early biocrust cyanobacterial species, *Microcoleus vaginatus*, is well adapted to moisture pulses and hot-dry conditions seen in the Warmed treatment of this experiment and is insensitive to altered climate (Ferrenberg and others 2015).

Bare Soil CO₂ Fluxes

In Bare soil mesocosms, respiration increased with warming during Wet and Moist phases, but not the Dry phase. From the beginning to end of the

experiment, R declined significantly and was very low by mid-November. This may represent either strong temperature sensitivity, or declining soil C availability, although measurements of soil C pools did not indicate a significant decline in total or dissolved soil C (total and 0.5 M K₂SO₄-extractable pools, data not shown). Nevertheless, Bare soil R was more sensitive to temperature than either Early or Late biocrust. There was no detectable C uptake in Bare soil mesocosms, indicating that during the course of the incubations they were not colonized by a substantial Early successional biocrust component. Furthermore, it indicates that soil inorganic carbonate formation was probably not a major carbon sink during the course of the experiment (Schlesinger 2017). We did not evaluate whether some of the soil CO₂ efflux was due to carbonate dissolution (Rey 2015) and suggest that this may be an important step for evaluating the complete soil C cycle in biocrusted soils.

Modeling Temperature and Moisture Sensitivity of Biocrusted Soil C Fluxes

In general, the model presented here fit the mesocosm data well. The fit for GPP was dominated by Late biocrusts; the model under-predicted the largest uptake events in Early biocrust (Figure 3). For Bare soil and Early biocrust, the endpoint cumulative fluxes (Figure 4) and time series of fluxes (Figure 5) largely reflected the mean measured fluxes under Wet, Moist, and Dry conditions (Figure 2). The Late biocrust time series of modeled cumulative fluxes, on the other hand, showed inhibition of R at night by dry conditions in the Warmed relative to Ambient mesocosms, which produced differences between the cumulative modeled fluxes and mean measured fluxes. Considering only daylight hours, the Late biocrust mesocosms under ambient temperatures were estimated to be a C sink during the cooler conditions present in November and December (Figure 5H). Yet considering both day and night, the Late Ambient mesocosms showed a similar cumulative C balance to the Late Warmed mesocosms. If this experiment continued all winter, we posit there would have been a larger shift toward C storage in the Ambient relative to Warmed mesocosms. This result is consistent with finding of Darrouzet-Nardi and others (2015) that substantial C uptake by Late biocrusted soils in field chambers occurred mostly during cool, moist periods.

The model broadly replicated patterns of NSE observed in CO₂ flux autochambers operating over patches of Late biocrust at the field site (Figure 8),

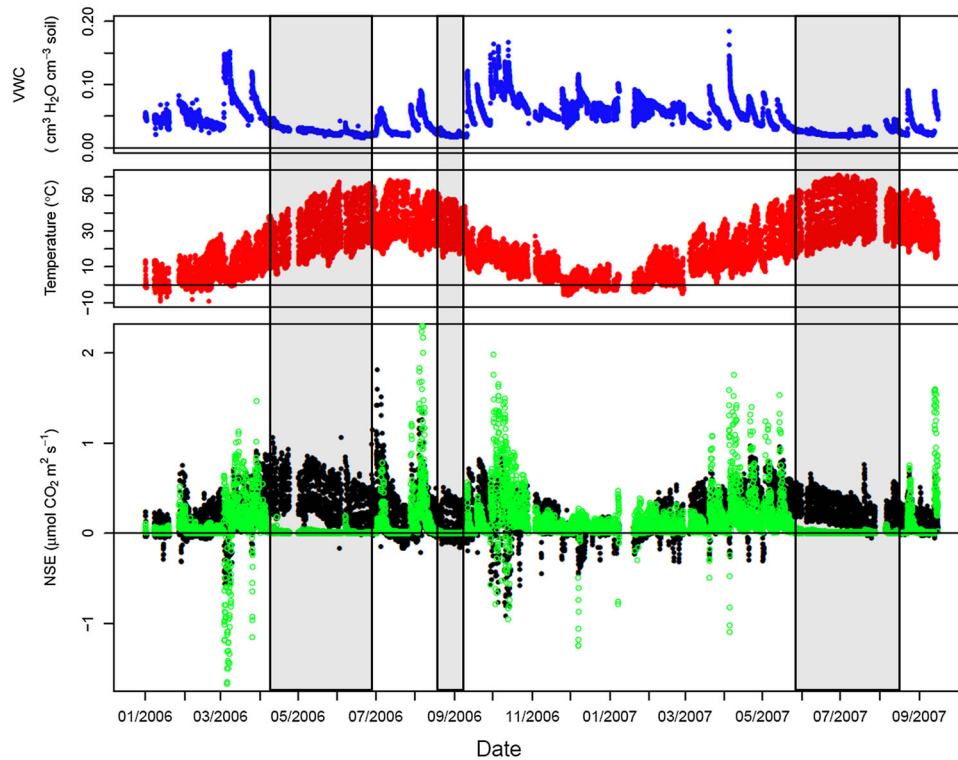


Figure 8. Soil moisture (blue), temperature (red), and net soil CO₂ exchange (NSE) of Late biocrust simulated from our model (Green) and measured (black) in the field using clear autochambers containing Late biocrust atop a soil profile at the same site from which the mesocosm specimens originated (black circles; Darrouzet-Nardi and others 2015). Autochamber data were collected hourly for a year and 7 months, and the autochambers collected data in both Ambient and Warmed plots (Warmed plots in the field were heated with infrared lamps and were kept at 2°C above ambient; detailed methods and results can be found in Darrouzet-Nardi and others 2015). The model showed a significant positive fit to the data ($r^2 = 0.136$, $p < 0.001$, supporting Figure 5) although the fit was fairly weak, driven by the time periods highlighted above.

which given the potential array of differences between greenhouse and field conditions (that is, wind advection, higher UV radiation, plant roots in the soil, deeper soils) was a surprising result. In general, pulsed patterns of high photosynthesis (negative NSE) and respiration (positive NSE) were replicated, and the overall magnitude was similar. However, there were several hot-dry periods (highlighted as gray boxes in Figure 8) where the model under-predicted CO₂ effluxes. The modeled moisture response seems intuitively realistic—low fluxes in dry soils, higher fluxes with wetter soils—while the high efflux at low soil moisture observed in the field data seems biologically less logical. Indeed, it has been documented that Late biocrust (in particular mosses) generally undergoes C loss with small wetting events (Coe and others 2012; Wu and others 2015), net C uptake with larger wetting events (Reed and others 2012) and little activity during drying periods. How then do we explain the difference between model and field

measurements, and the high rates of soil CO₂ exchange at low moistures in the field? One explanation is that field soil moisture sensors do not capture biocrust surface moisture when precipitation or dew formation wet biocrust but not deeper soils. This could result in biocrust CO₂ efflux when subsoils (where the soil moisture sensors are located) are dry (Tucker and others 2017). Biocrust surface moisture measurements, or a model [such as presented by (Wilske and others 2009)] that includes relative humidity, would improve our ability to model this relationship, particularly when considering anatomical adaptations for collection of non-rainfall moisture in biocrust mosses (Pan and others 2016). Other under-explored possible sources of CO₂ efflux include expansion of soil gas with warming (Rey 2015), carbonate dissolution (Schlesinger 2017), or root respiration in the soil beneath the autochamber. Work partitioning these potential fluxes in the field would be of great value.

Several assumptions built into the model merit testing and will require model improvement. We assumed the relationship between R and environmental conditions is the same at night, in the absence of C fixation, as during the daylight. Although this assumption is reasonable for Bare soil fluxes, in biocrusted mesocosms differences in C substrate (that is, new photosynthate) availability may result in different relationships of fluxes to environmental conditions between night and day. In Figure 7, we indicate that R_g shows the same temperature and moisture sensitivity in Bare soil as under both Early and Late crust, yet coupling of the C cycle between biocrust and the soil beneath may change these relationships. Further, changes in C availability or quality (Fierer and others 2005) or thermal acclimation (Luo and others 2001; Atkin and Tjoelker 2003; Tucker and others 2013) may have occurred in ways our model did not capture. Finally, the model presented here is not yet a viable tool for predicting ecosystem C balance because more C could potentially be lost than is present in the system over long periods of time with the current simple model structure (for example, without vascular plants, key soil C inputs are missing). Thus, a more fully realized process model (including mass balance constraints) will be necessary for making long-term projections of ecosystem change.

A Climate Change-C Cycle Integrated Framework for Biocrusted Drylands

Taken together, the data suggest that warming-induced changes to C cycling in biocrusted ecosystems interact with biocrust successional state in ways that may have substantial impacts on the ecosystem C balance. These changes appear to be largely mediated through soil water content, as warming accelerates soil drying. Modeled cumulative fluxes also suggest that seasonal patterns of temperature sensitivity are important to consider when evaluating and predicting the consequences of climate warming, especially in the Late biocrust, which these data indicate is the dominant contributor to C cycling in biocrusted interspaces in this system. We suggest three particularly important future research directions: (1) developing regional scale assessments of biocrust cover and species composition in drylands, (2) contextualizing biocrust contributions to CO₂ exchange with those from vascular plants, and (3) integrating biocrusts into ecosystem and Earth system models, so that quantitative estimates of changes in biocrust C cycling are possible. When we consider the syn-

ergistic effects of climate change on dryland biocrust activity and successional state, the potential for dramatic declines in biome-scale C cycling rates over the coming decades emerges as biocrust communities respond to warming.

ACKNOWLEDGEMENTS

This material is based upon work supported by US Department of Energy Office of Science, Office of Biological and Environmental Research Terrestrial Ecosystem Sciences Program, under Award Number DE-SC-0008168 and by US Geological Survey Ecosystems Mission Area. We appreciate everyone who worked on this project, especially Armin Howell, Robin Reibold, Rose Egelhoff and Paige Austin. We thank Anthony Darrouzet-Nardi for valuable feedback on the manuscript. Any use of trade, firm, or product names is for descriptive purposes only and does not imply endorsement by the US Government.

REFERENCES

- Ahlström A, Raupach MR, Schurgers G, Smith B, Arneth A, Jung M, Reichstein M, Canadell JG, Friedlingstein P, Jain AK, Kato E, Poulter B, Sitch S, Stocker BD, Viovy N, Wang YP, Wiltshire A, Zaehle S, Zeng N. 2015. The dominant role of semi-arid ecosystems in the trend and variability of the land CO₂ sink. *Science* 348:895–9.
- Atkin OK, Tjoelker MG. 2003. Thermal acclimation and the dynamic response of plant respiration to temperature. *Trends in plant science* 8:343–51.
- Austin A, Yahdjian L, Stark J, Belnap J, Porporato A, Norton U, Ravetta D, Schaeffer S. 2004. Water pulses and biogeochemical cycles in arid and semiarid ecosystems. *Oecologia* 141:221–35.
- Barger NN, Weber B, Garcia-Pichel F, Zaady E, Belnap J. 2016. Patterns and controls on nitrogen cycling of biological soil crusts. *Biological soil crusts: an organizing principle in drylands*. Berlin: Springer. pp 257–85.
- Belnap J. 1995. Surface disturbances: their role in accelerating desertification. *Desertification in developed countries*. Berlin: Springer. pp 39–57.
- Belnap J. 2002. Nitrogen fixation in biological soil crusts from southeast Utah, USA. *Biol Fertil Soils* 35:128–35.
- Belnap J, Phillips SL, Miller ME. 2004. Response of desert biological soil crusts to alterations in precipitation frequency. *Oecologia* 141:306–16.
- Belnap J, Weber B, Büdel B. 2016. Biological soil crusts as an organizing principle in drylands. *Biological soil crusts: an organizing principle in drylands*. Berlin: Springer. pp 3–13.
- Bowker MA, Belnap J, Büdel B, Sannier C, Pietrasiak N, Eldridge DJ, Rivera-Aguilar V. 2016. Controls on distribution patterns of biological soil crusts at micro-to global scales. *Biological soil crusts: an organizing principle in drylands*. Berlin: Springer. pp 173–97.
- Bowker MA, Maestre FT, Eldridge D, Belnap J, Castillo-Monroy A, Escolar C, Soliveres S. 2014. Biological soil crusts (bio-

- crusts) as a model system in community, landscape and ecosystem ecology. *Biodivers Conserv* 23:1619–37.
- Bowker MA, Mau RL, Maestre FT, Escolar C, Castillo-Monroy AP. 2011. Functional profiles reveal unique ecological roles of various biological soil crust organisms. *Funct Ecol* 25:787–95.
- Burgheimer J, Wilske B, Maseyk K, Karnieli A, Zaady E, Yakir D, Kesselmeier J. 2006. Relationships between normalized difference vegetation index (NDVI) and carbon fluxes of biologic soil crusts assessed by ground measurements. *J Arid Environ* 64:651–69.
- Castillo-Monroy AP, Bowker MA, Maestre FT, Rodriguez-Echeverria S, Martinez I, Barraza-Zepeda CE, Escolar C. 2011a. Relationships between biological soil crusts, bacterial diversity and abundance, and ecosystem functioning: Insights from a semi-arid Mediterranean environment. *J Veg Sci* 22:165–74.
- Castillo-Monroy AP, Maestre FT, Rey A, Soliveres S, Garcia-Palacios P. 2011b. Biological soil crust microsites are the main contributor to soil respiration in a semiarid ecosystem. *Ecosystems* 14:835–47.
- Coe KK, Belnap J, Sparks JP. 2012. Precipitation-driven carbon balance controls survivorship of desert biocrust mosses. *Ecology* 93:1626–36.
- Couradeau E, Karaoz U, Lim HC, da Rocha UN, Northen T, Brodie E, Garcia-Pichel F. 2016. Bacteria increase arid-land soil surface temperature through the production of sunscreens. *Nat Commun* 7:10373.
- Darrouzet-Nardi A, Reed SC, Grote EE, Belnap J. 2015. Observations of net soil exchange of CO₂ in a dryland show experimental warming increases carbon losses in biocrust soils. *Biogeochemistry* 126:363–78.
- Delgado-Baquerizo M, Maestre FT, Gallardo A, Bowker MA, Wallenstein MD, Quero JL, Ochoa V, Gozalo B, Garcia-Gomez M, Soliveres S, Garcia-Palacios P, Berdugo M, Valencia E, Escolar C, Arredondo T, Barraza-Zepeda C, Bran D, Carreira JA, Chaieb M, Conceicao AA, Derak M, Eldridge DJ, Escudero A, Espinosa CI, Gaitan J, Gatica MG, Gomez-Gonzalez S, Guzman E, Gutierrez JR, Florentino A, Hepper E, Hernandez RM, Huber-Sannwald E, Jankju M, Liu J, Mau RL, Miriti M, Moneris J, Naseri K, Noumi Z, Polo V, Prina A, Pucheta E, Ramirez E, Ramirez-Collantes DA, Romao R, Tighe M, Torres D, Torres-Diaz C, Ungar ED, Val J, Wamiti W, Wang D, Zaady E. 2013. Decoupling of soil nutrient cycles as a function of aridity in global drylands. *Nature* 502:672–6.
- Delgado-Baquerizo M, Gallardo A, Covelos F, Prado-Comesaña A, Ochoa V, Maestre FT. 2015. Differences in thallus chemistry are related to species-specific effects of biocrust-forming lichens on soil nutrients and microbial communities. *Funct Ecol* 29:1087–98.
- Elbert W, Weber B, Burrows S, Steinkamp J, Budel B, Andreae MO, Poschl U. 2012. Contribution of cryptogamic covers to the global cycles of carbon and nitrogen. *Nat Geosci* 5:459–62.
- Escolar C, Maestre FT, Rey A. 2015. Biocrusts modulate warming and rainfall exclusion effects on soil respiration in a semi-arid grassland. *Soil Biol Biochem* 80:9–17.
- Ferrenberg S, Faist AM, Howell A, Reed SC. 2017a. Biocrusts enhance soil fertility and *Bromus tectorum* growth, and interact with warming to influence germination. *Plant Soil*. <https://doi.org/10.1007/s11104-017-3525-1>.
- Ferrenberg S, Reed SC, Belnap J. 2015. Climate change and physical disturbance cause similar community shifts in biological soil crusts. *Proc Natl Acad Sci* 112:12116–21.
- Ferrenberg S, Tucker CL, Reed SC. 2017b. Biological soil crusts: diminutive communities of potential global importance. *Fron Ecol Environ* 15(3):160–7.
- Fierer N, Craine JM, McLaughlan K, Schimel JP. 2005. Litter quality and the temperature sensitivity of decomposition. *Ecology* 86:320–6.
- Garcia-Pichel F, Johnson SL, Youngkin D, Belnap J. 2003. Small-scale vertical distribution of bacterial biomass and diversity in biological soil crusts from arid lands in the Colorado Plateau. *Microb Ecol* 46:312–21.
- Green TA, Proctor MC. 2016. Physiology of photosynthetic organisms within biological soil crusts: their adaptation, flexibility, and plasticity. *biological soil crusts: an organizing principle in drylands*. Berlin: Springer. pp 347–81.
- Grote EE, Belnap J, Housman DC, Sparks JP. 2010. Carbon exchange in biological soil crust communities under differential temperatures and soil water contents: implications for global change. *Global Change Biol* 16:2763–74.
- Housman DC, Powers HH, Collins AD, Belnap J. 2006. Carbon and nitrogen fixation differ between successional stages of biological soil crusts in the Colorado Plateau and Chihuahuan Desert. *J Arid Environ* 66:620–34.
- Janssens IA, Kowalski AS, Ceulemans R. 2001. Forest floor CO₂ fluxes estimated by eddy covariance and chamber-based model. *Agric Forest Meteorol* 106:61–9.
- Jasoni RL, Smith SD, Arnone JA. 2005. Net ecosystem CO₂ exchange in Mojave Desert shrublands during the eighth year of exposure to elevated CO₂. *Global Change Biol* 11:749–56.
- Kizito F, Campbell CS, Campbell GS, Cobos DR, Teare BL, Carter B, Hopmans JW. 2008. Frequency, electrical conductivity and temperature analysis of a low-cost capacitance soil moisture sensor. *J Hydrol* 352:367–78.
- Klos PZ, Link TE, Abatzoglou JT. 2014. Extent of the rain-snow transition zone in the western U.S. under historic and projected climate. *Geophys Res Lett* 41:4560–8.
- Lange O, Belnap J, Lange O. 2003. Photosynthesis of soil-biota as dependent on environmental factors. *Biol Soil Crusts: Struct Funct Manag* 349–360.
- Lange OL, Green TA, Heber U. 2001. Hydration-dependent photosynthetic production of lichens: what do laboratory studies tell us about field performance? *J Exp Bot* 52:2033–42.
- Li XR, Zhang P, Su YG, Jia RL. 2012. Carbon fixation by biological soil crusts following revegetation of sand dunes in arid desert regions of China: a four-year field study. *Catena* 97:119–26.
- Lloyd J, Taylor JA. 1994. On the temperature dependence of soil respiration. *Funct Ecol* 8:315–23.
- Luo Y, Wan S, Hui D, Wallace LL. 2001. Acclimatization of soil respiration to warming in a tall grass prairie. *Nature* 413:622–5.
- Maestre FT, Bowker MA, Eldridge DJ, Cortina J, Lázaro R, Gallardo A, Delgado-Baquerizo M, Berdugo M, Castillo-Monroy AP, Valencia E. 2016. Biological soil crusts as a model system in ecology. *biological soil crusts: an organizing principle in drylands*. Berlin: Springer. pp 407–25.
- Maestre FT, Castillo-Monroy AP, Bowker MA, Ochoa-Hueso R. 2012a. Species richness effects on ecosystem multifunctionality depend on evenness, composition and spatial pattern. *J Ecol* 100:317–30.
- Maestre FT, Escolar C, de Guevara ML, Quero JL, Lázaro R, Delgado-Baquerizo M, Ochoa V, Berdugo M, Gozalo B, Gallardo A. 2013. Changes in biocrust cover drive carbon cycle

- responses to climate change in drylands. *Global Change Biol* 19:3835–47.
- Maestre FT, Salguero-Gómez R, Quero JL. 2012b. It is getting hotter in here: determining and projecting the impacts of global environmental change on drylands. *Philos Trans R Soc Lond B Biol Sci* 367(1606):3062–75.
- Marschall M, Proctor MC. 2004. Are bryophytes shade plants? Photosynthetic light responses and proportions of chlorophyll a, chlorophyll b and total carotenoids. *Ann Bot* 94:593–603.
- McHugh TA, Morrissey EM, Reed SC, Hungate BA, Schwartz E. 2015. Water from air: an overlooked source of moisture in arid and semiarid regions. *Sci Rep* 5:13767.
- Ogle K, Barber JJ. 2008. Bayesian data—model integration in plant physiological and ecosystem ecology. *Progress in botany*. Berlin: Springer. pp 281–311.
- Pan Z, Pitt WG, Zhang Y, Wu N, Tao Y, Truscott TT. 2016. The upside-down water collection system of *Syntrichia caninervis*. *Nat Plants* 2:16076.
- Pendleton RL, Pendleton BK, Howard GL, Warren SD. 2003. Growth and nutrient content of herbaceous seedlings associated with biological soil crusts. *Arid Land Res Manag* 17:271–81.
- Pointing SB, Belnap J. 2014. Disturbance to desert soil ecosystems contributes to dust-mediated impacts at regional scales. *Biodivers Conserv* 23:1659–67.
- Poulter B, Frank D, Ciais P, Myneni RB, Andela N, Bi J, Broquet G, Canadell JG, Chevallier F, Liu YY, Running SW, Sitch S, van der Werf GR. 2014. Contribution of semi-arid ecosystems to interannual variability of the global carbon cycle. *Nature* 509:600–3.
- Raich J, Rastetter E, Melillo J, Kicklighter D, Stuedler P, Peterson B, Grace A, Moore B, Vorosmarty C. 1991. Potential net primary productivity in North America: application of a global model. *Ecol Appl* 1:399–429.
- Reed SC, Coe KK, Sparks JP, Housman DC, Zelikova TJ, Belnap J. 2012. Changes to dryland rainfall result in rapid moss mortality and altered soil fertility. *Nat Clim Change* 2:752–5.
- Reed SC, Maestre FT, Ochoa-Hueso R, Kuske CR, Darrouzet-Nardi A, Oliver M, Darby B, Sancho LG, Sinsabaugh RL, Belnap J. 2016. Biocrusts in the Context of Global Change. In: Weber B, Büdel B, Belnap J, Eds. *Biological soil crusts: an organizing principle in drylands*. Cham: Springer. p 451–76.
- Rey A. 2015. Mind the gap: non-biological processes contributing to soil CO₂ efflux. *Global Change Biol* 21:1752–61.
- Rutherford WA, Painter TH, Ferrenberg S, Belnap J, Okin GS, Flagg C, Reed SC. 2017. Albedo feedbacks to future climate via climate change impacts on dryland biocrusts. *Sci Rep* 7:44188.
- Safriel U, Adeel Z. 2005. Drylands. Chapter 22 of millennium ecosystem assessment. Washington, DC: Island Press.
- Sancho LG, Belnap J, Colesie C, Raggio J, Weber B. 2016. Carbon budgets of biological soil crusts at micro-, meso-, and global scales: an organizing principle in drylands. Berlin: Springer. pp 287–304.
- Schimel DS. 2010. Drylands in the earth system. *Science* 327:418–19.
- Schlesinger WH. 2017. An evaluation of abiotic carbon sinks in deserts. *Global Change Biol* 23:25–7.
- Schlesinger WH, Belnap J, Marion G. 2009. On carbon sequestration in desert ecosystems. *Global Change Biol* 15:1488–90.
- Strickland MS, Lauber C, Fierer N, Bradford MA. 2009. Testing the functional significance of microbial community composition. *Ecology* 90:441–51.
- Thomas AD, Hoon SR, Dougill AJ. 2011. Soil respiration at five sites along the Kalahari transect: effects of temperature, precipitation pulses and biological soil crust cover. *Geoderma* 167–68:284–94.
- Torres-Cruz TJ, Howell AJ, Reibold RH, McHugh TA, Eickhoff MA, Reed SC. 2018. Species-specific nitrogenase activity in lichen-dominated biological soil crusts from the Colorado Plateau, USA. *Plant Soil*. <https://doi.org/10.1007/s11104-018-3580-2>.
- Tucker CL, Bell J, Pendall E, Ogle K. 2013. Does declining carbon-use efficiency explain thermal acclimation of soil respiration with warming? *Global Change Biol* 19:252–63.
- Tucker CL, McHugh TA, Howell A, Gill R, Weber B, Belnap J, Grote E, Reed SC. 2017. The concurrent use of novel soil surface microclimate measurements to evaluate CO₂ pulses in biocrusted interspaces in a cool desert ecosystem. *Biogeochemistry* 135:239–49.
- Tucker CL, Reed SC. 2016. Low soil moisture during hot periods drives apparent negative temperature sensitivity of soil respiration in a dryland ecosystem: a multi-model comparison. *Biogeochemistry* 128:155–69.
- Weber B, Bowker M, Zhang Y, Belnap J. 2016. Natural recovery of biological soil crusts after disturbance. *Biological soil crusts: an organizing principle in drylands*. Berlin: Springer. pp 479–98.
- Weber B, Wu D, Tamm A, Ruckteschler N, Rodríguez-Caballero E, Steinkamp J, Meusel H, Elbert W, Behrendt T, Sörgel M, Cheng Y, Crutzen PJ, Su H, Pöschl U. 2015. Biological soil crusts accelerate the nitrogen cycle through large NO and HONO emissions in drylands. *Proc Natl Acad Sci* 112:15384–9.
- Wertin T, Reed S, Belnap J. 2015. C₃ and C₄ plant responses to increased temperatures and altered monsoonal precipitation in a cool desert on the Colorado Plateau, USA. *Oecologia* 177:997–1013.
- Wilske B, Burgheimer J, Karnieli A, Zaady E, Andreae M, Yakir D, Kesselmeier J. 2008. The CO₂ exchange of biological soil crusts in a semiarid grass-shrubland at the northern transition zone of the Negev desert, Israel. *Biogeosci Discuss* 5:1969–2001.
- Wilske B, Burgheimer J, Maseyk K, Karnieli A, Zaady E, Andreae M, Yakir D, Kesselmeier J. 2009. Modeling the variability in annual carbon fluxes related to biological soil crusts in a Mediterranean shrubland. *Biogeosci Discuss* 6:7295–324.
- Wohlfahrt G, Fenstermaker LF, Arnone Iii JA. 2008. Large annual net ecosystem CO₂ uptake of a Mojave Desert ecosystem. *Global Change Biol* 14:1475–87.
- Wu L, Zhang YM, Zhang J, Downing A. 2015. Precipitation intensity is the primary driver of moss crust-derived CO₂ exchange: Implications for soil C balance in a temperate desert of northwestern China. *Eur J Soil Biol* 67:27–34.
- Zaady E, Kuhn U, Wilske B, Sandoval-Soto L, Kesselmeier J. 2000. Patterns of CO₂ exchange in biological soil crusts of successional age. *Soil Biol Biochem* 32:959–66.
- Zhang Y, Aradottir AL, Serpe M, Boeken B. 2016. Interactions of biological soil crusts with vascular plants. *Biological soil crusts: an organizing principle in drylands*. Berlin: Springer. pp 385–406.
- Zhao Y, Zhang ZS, Hu YG, Chen YL. 2016. The seasonal and successional variations of carbon release from biological soil crust-covered soil. *J Arid Environ* 127:148–53.